

Draft: January 22, 2007

# Constraints on Dark Energy from Supernovae, $\gamma$ -ray bursts, Acoustic Oscillations, Nucleosynthesis and Large Scale Structure and the Hubble constant

E. L. Wright<sup>1</sup>,

wright@astro.ucla.edu

## ABSTRACT

The luminosity distance *vs.* redshift law is now measured using supernovae and  $\gamma$ -ray bursts, and the angular size distance is measured at the surface of last scattering by the CMB and at  $z = 0.35$  by baryon acoustic oscillations. In this paper this data is fit to models for the equation of state with  $w = -1$ ,  $w = \text{constant}$ , and  $w(z) = w_0 + w_a(1 - a)$ . The last model is poorly constrained by the distance data, leading to unphysical solutions where the dark energy dominates at early times unless the large scale structure and acoustic scale constraints are modified to allow for early time dark energy effects. A flat  $\Lambda$ CDM model is consistent with all the data.

*Subject headings:* cosmic microwave background, cosmology: observations, early universe, dark matter

## 1. INTRODUCTION

Wood-Vasey *et al.* (2007) recently published supernova data from the ESSENCE project, while Riess *et al.* have published a large sample of supernovae from the SNLS project (Astier *et al.* 2006), the HST, and Hi-z Supernova Team. Schaefer (2007) has published a sample of  $\gamma$ -ray burst distances. While GRBs give much less accurate distances than supernovae, they extend to much higher redshifts and the GRB data helps to distinguish between non-flat geometries and equations of state with  $w \neq -1$  which both affect the distance-redshift law at  $\mathcal{O}(z^3)$  for low redshift.

---

<sup>1</sup>UCLA Astronomy, PO Box 951547, Los Angeles CA 90095-1547, USA

Barger *et al.* (2006) have analyzed the Riess *et al.* (2007) dataset, but not the GRBs or the ESSENCE dataset.

The analysis of Wood-Vasey *et al.* (2007) plotted contours of  $w$  and  $w_a$ , based only on a subset of the supernova data used here and a prior on  $\Omega_M$ . These contours extended into the region where the dark energy dominated the density at the surface of last scattering or during nucleosynthesis. Both Barger *et al.* (2006) and Riess *et al.* (2007) used  $w(z)$  laws in which the variation was terminated for  $z > 1.8$ , beyond the redshift of the most distant supernova in the sample, but this is an arbitrary limit which would have to be modified to allow for GRBs. Davis *et al.* (2007) have analyzed a subset of the combined supernovae, and have used an approximation to the CMB acoustic peak constraint that fails when dark energy dominates at high  $z$ . The part of parameter space where dark energy dominates at high  $z$  obviously should be excluded, and I show in this paper that appropriate modifications to the standard formulae for the acoustic scale, the  $\Gamma$  parameter, and Big Bang nucleosynthesis to allow for the possible importance of dark energy at  $z \approx 10^9$  or  $z \approx 10^3$  will lead to this exclusion automatically.

## 2. OBSERVATIONS

### 2.1. Supernovae

The distance modulus *vs.* redshift data from Riess *et al.* (2007) were taken from the Web site provided by Riess. The distance moduli and redshifts for the ESSENCE supernovae were extracted from Table 9 in the Latex file for astro-ph/0701041 (Wood-Vasey *et al.* 2007). Typically different groups analyze supernovae with different assumptions about the Hubble constant or equivalently the absolute magnitude  $\mathcal{M}$  of a canonical SN Ia with a nominal decay rate. In order to combine the new supernovae from ESSENCE with the Riess *et al.* sample, it was necessary to check the relative normalization of the two data sets using the 93 objects they have in common. Figure 1 shows the comparison. The scatter in the differential distance moduli is 0.2 mag  $1\sigma$ , which seems unusually high, and the median difference in  $\mu$  is 0.022 mag which is consistent with the standard deviation of the mean given the scatter. Objects which are not in the Riess *et al.* sample but which had successful fits with  $\chi^2$  per degree of freedom  $< 7$  were added to the Riess *et al.* sample, with the 0.022 mag added to  $\mu$ , and an intrinsic scatter of 0.10 mag added in quadrature to  $\sigma_\mu$ . This gives a total sample of 358 SNe. I have binned the SNe into bins containing  $< 2 + N_{tot}/10$  objects and widths less than 0.1 in redshift. An empty Universe model (the Milne model) was first subtracted from the  $\mu$  values. The binned values are listed in Table 1. A Hubble constant of 63.8 km/sec/Mpc was used when computing the Milne model, but this value has no effect on

$\langle z \rangle$	$\langle \Delta\mu \rangle$	$z_{min}$	$z_{max}$	$N$
0.0159	$-0.052 \pm 0.118$	0.007	0.024	37
0.0376	$0.004 \pm 0.057$	0.024	0.058	37
0.0947	$0.103 \pm 0.075$	0.061	0.160	12
0.2207	$0.110 \pm 0.062$	0.172	0.268	14
0.3299	$0.096 \pm 0.037$	0.274	0.371	36
0.4222	$0.170 \pm 0.037$	0.374	0.455	37
0.4841	$0.245 \pm 0.037$	0.459	0.511	37
0.5530	$0.169 \pm 0.034$	0.514	0.610	37
0.6550	$0.100 \pm 0.036$	0.612	0.710	31
0.7747	$0.054 \pm 0.053$	0.719	0.818	21
0.8590	$0.055 \pm 0.064$	0.822	0.910	20
0.9661	$0.047 \pm 0.068$	0.927	1.020	21
1.1140	$0.017 \pm 0.118$	1.056	1.140	4
1.2228	$-0.087 \pm 0.127$	1.190	1.265	5
1.3353	$-0.151 \pm 0.100$	1.300	1.390	6
1.4000	$0.037 \pm 0.810$	1.400	1.400	1
1.5510	$-0.490 \pm 0.320$	1.551	1.551	1
1.7550	$-0.599 \pm 0.350$	1.755	1.755	1

Table 1: Mean distance modulus relative to a Milne model for the 358 supernovae in Riess *et al.* (2007) Gold+Silver and Wood-Vasey *et al.* (2007).

the parameter limits computed in this paper. Its only effect is to add a constant to the  $\langle \Delta\mu \rangle$  values in the Tables. The mean differential distance modulus in each bin is found by minimizing a modified

$$\chi^2 = \sum_i f((\langle \Delta\mu \rangle - [\mu_i - \mu_{Milne}])/\sigma_i) \quad (1)$$

where  $f(x) = x^2$  for  $|x| < 2$ , or  $4|x| - 4$  otherwise. The modification deweights extreme outliers. Riess *et al.* (2007) recommend dropping SNe with redshifts less than 0.023 to avoid a possible “Hubble bubble” seen by Jha *et al.* (2007), but I have instead used a large velocity error of  $\sigma_v = 1500$  km/sec which gives an extra  $\sigma_\mu$  of  $(5/\ln 10)(\sigma_v/cz)$  which is added in quadrature with the tabulated  $\sigma_\mu$ .

Table 2 was constructed the same way but omitting the “Silver” objects in Riess *et al.* (2007).

The binned values from Tables 1 and 2 are shown in Figure 2 along with the flat  $\Lambda$ CDM

$\langle z \rangle$	$\langle \Delta\mu \rangle$	$z_{min}$	$z_{max}$	$N$
0.0169	$-0.035 \pm 0.125$	0.010	0.025	29
0.0361	$0.024 \pm 0.067$	0.025	0.053	29
0.0776	$0.074 \pm 0.080$	0.056	0.124	10
0.2032	$0.123 \pm 0.073$	0.159	0.249	10
0.3196	$0.105 \pm 0.042$	0.263	0.363	27
0.4149	$0.144 \pm 0.039$	0.368	0.450	29
0.4808	$0.203 \pm 0.040$	0.455	0.508	29
0.5514	$0.139 \pm 0.039$	0.510	0.604	29
0.6475	$0.119 \pm 0.038$	0.610	0.707	25
0.7888	$0.058 \pm 0.059$	0.730	0.830	18
0.8666	$0.007 \pm 0.081$	0.832	0.905	10
0.9696	$0.035 \pm 0.076$	0.935	1.020	14
1.1140	$0.017 \pm 0.118$	1.056	1.140	4
1.2197	$0.081 \pm 0.143$	1.199	1.230	3
1.3410	$-0.163 \pm 0.105$	1.300	1.390	5
1.7550	$-0.599 \pm 0.350$	1.755	1.755	1

Table 2: Mean distance modulus relative to a Milne model for 272 supernovae in Riess *et al.* (2007) Gold and Wood-Vasey *et al.* (2007).

model that best fits the Hubble diagram data alone. This model has  $\Omega_M = 0.369$ . There is an excursion around  $z = 0.5$  that can be seen clearly in the binned supernova data. A simple 3 parameter fit to this bump gives a  $\Delta\chi^2$  of 15 in the total sample, but only 6 if the “Silver” SNe are excluded.

## 2.2. GRBs

Schaefer (2007) has given a sample of 69 GRBs with redshifts and distance moduli. These values have been binned as well, but with bin widths  $< 0.1(1+z_{min}+z_{max})$ . The binned values are listed in Table 3. In constructing the Table, a Milne model with a Hubble constant of 72 km/sec/Mpc was subtracted from the individual distance moduli before minimizing the modified  $\chi^2$ . Figure 3 shows the binned data from both the GRBs and the supernovae.

$\langle z \rangle$	$\langle \Delta\mu \rangle$	$z_{min}$	$z_{max}$	$N$
0.2100	$0.453 \pm 0.362$	0.170	0.250	2
0.4967	$0.458 \pm 0.289$	0.430	0.610	3
0.7350	$0.479 \pm 0.217$	0.650	0.830	8
0.9187	$-0.090 \pm 0.171$	0.840	1.020	8
1.2083	$0.173 \pm 0.263$	1.060	1.310	6
1.5275	$-0.202 \pm 0.175$	1.440	1.620	8
2.0217	$-0.141 \pm 0.257$	1.710	2.200	6
2.4825	$-0.117 \pm 0.211$	2.300	2.680	8
3.1463	$-0.785 \pm 0.215$	2.820	3.370	8
3.8243	$-0.573 \pm 0.247$	3.420	4.270	7
4.6033	$-0.946 \pm 0.412$	4.410	4.900	3
6.4450	$-1.100 \pm 0.463$	6.290	6.600	2

Table 3: Mean distance modulus relative to a Milne model for 69 GRBs in Schaefer (2007).

### 2.3. Hubble Constant

The Hubble constant largely cancels out in analyses of supernovae and  $\gamma$ -ray burst distances. But the Hubble constant does enter into converting the  $\Gamma$  parameter ( $\Omega_M h$ ) into a prior on  $\Omega_M$ . The Hubble constant data used in this paper comes from Freedman *et al.* (2001), the DIRECT project double-lined eclipsing binary in M33 (Bonanos *et al.* 2006), Cepheids in the nuclear maser ring galaxy M106 (Macri *et al.* 2006), and the Sunyaev-Zeldovich effect (Bonamente *et al.* 2006). These papers gave values of  $72 \pm 8$ ,  $61 \pm 4$ ,  $74 \pm 7$  and  $77 \pm 10$  km/sec/Mpc. Assuming that the uncertainties in these determinations are uncorrelated and equal to 10 km/sec/Mpc after allowing for systematics, the average value for  $H_0$  is  $71 \pm 5$  km/sec/Mpc.

### 2.4. Matter Density

The matter density  $\Omega_M h^2$  is fairly well determined by fitting the CMB power spectrum. In this paper the non-flat  $\Lambda$ CDM chain (ocdm\_wmap\_1.txt) at the LAMBDA data center has been used to determine average values for parameters. This chain gives  $\omega_M = \Omega_M h^2 = 0.1289 \pm 0.0079$ . The baryonic density is also well determined, with  $\omega_B = \Omega_B h^2 = 0.02178 \pm 0.00072$ .

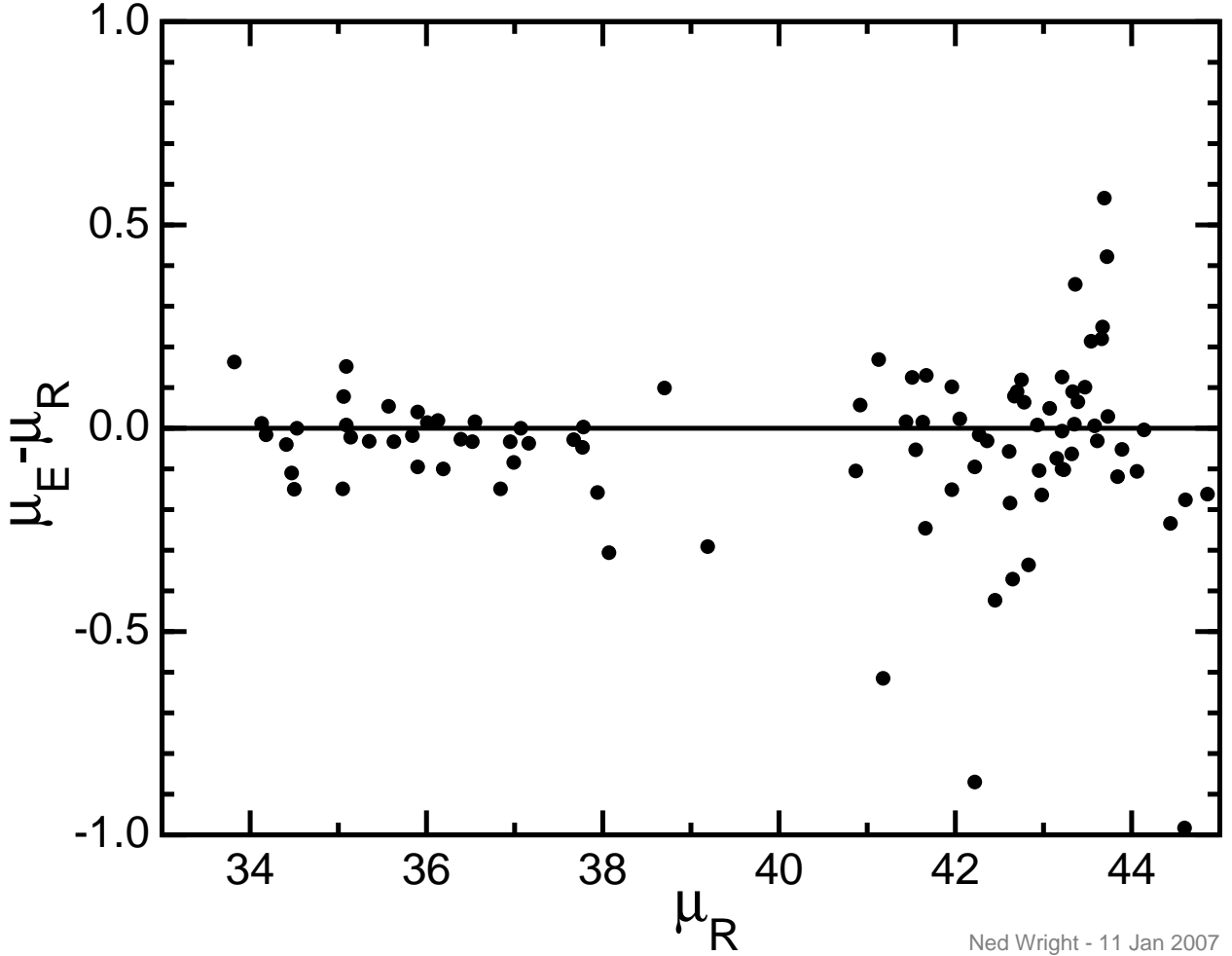


Fig. 1.— Difference in distance moduli for objects common to Wood-Vasey *et al.* (2007) ( $\mu_E$ ) and Riess *et al.* (2007) ( $\mu_R$ ). The RMS scatter is 0.2 mag.

## 2.5. Large Scale Structure

Large scale structure data comes from the “big bend” in the power spectrum  $P(k)$ . This has been measured by two large galaxy surveys: the SDSS and the 2dF. The SDSS gives a value for  $\Gamma = \Omega_M h = 0.213 \pm 0.0233$  (Tegmark *et al.* 2004), while the 2dF gives (Cole *et al.* 2005)

$$\Omega_M h = \Gamma_{true} = 0.168 \pm 0.016 + 0.3(1 - n_s) + 1.2\Omega_\nu/\Omega_M \quad (2)$$

I assume that the Tegmark *et al.* value uses  $n_s = 1$  and  $\Omega_\nu = 0$ , and that it has the same sensitivity to these parameters as the 2dF. The combination of these two values gives a  $\chi^2 = 2.6$  for 1 degree of freedom. While this is higher than the expected value of 1, it is certainly not high enough to trigger grave concerns. The neutrino density is uncertain but

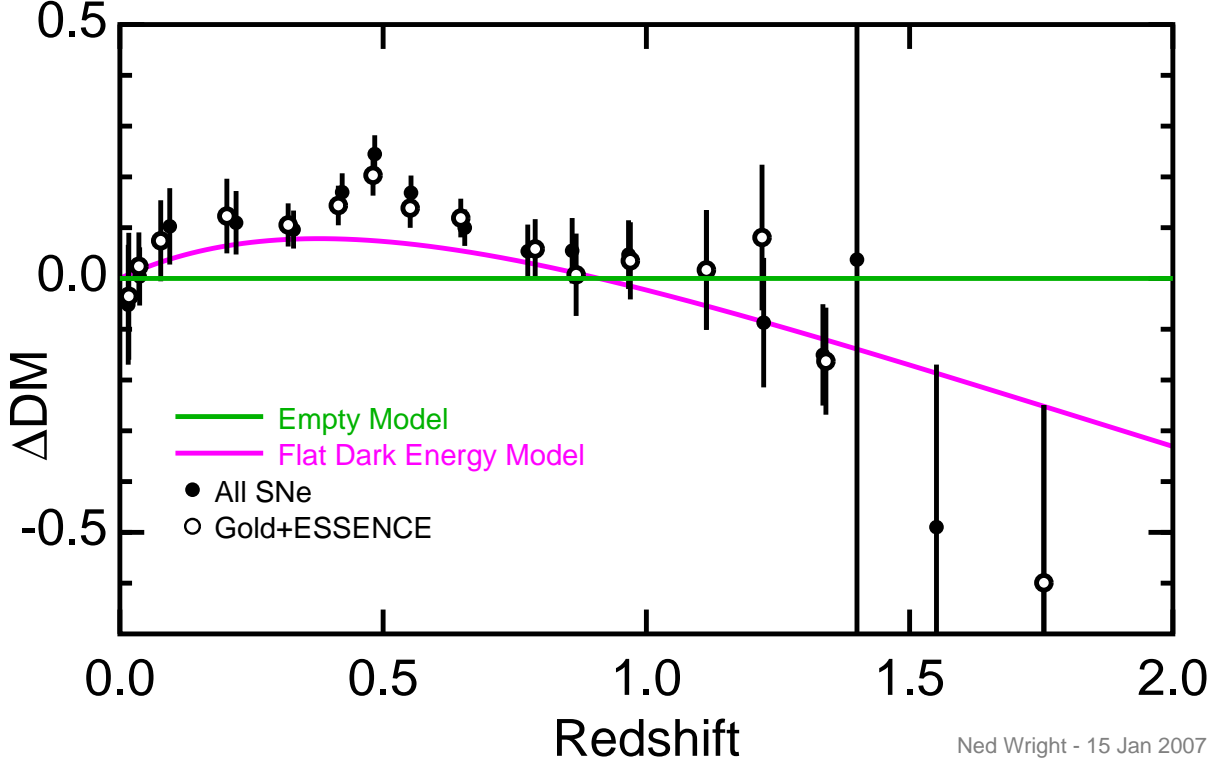


Fig. 2.— Binned supernova data *vs.* redshift compared to a flat  $\Lambda$ CDM model with  $\Omega_M = 0.369$ . The filled circles are binned points from the full dataset, while the open circles have omitted the “Silver” subset.

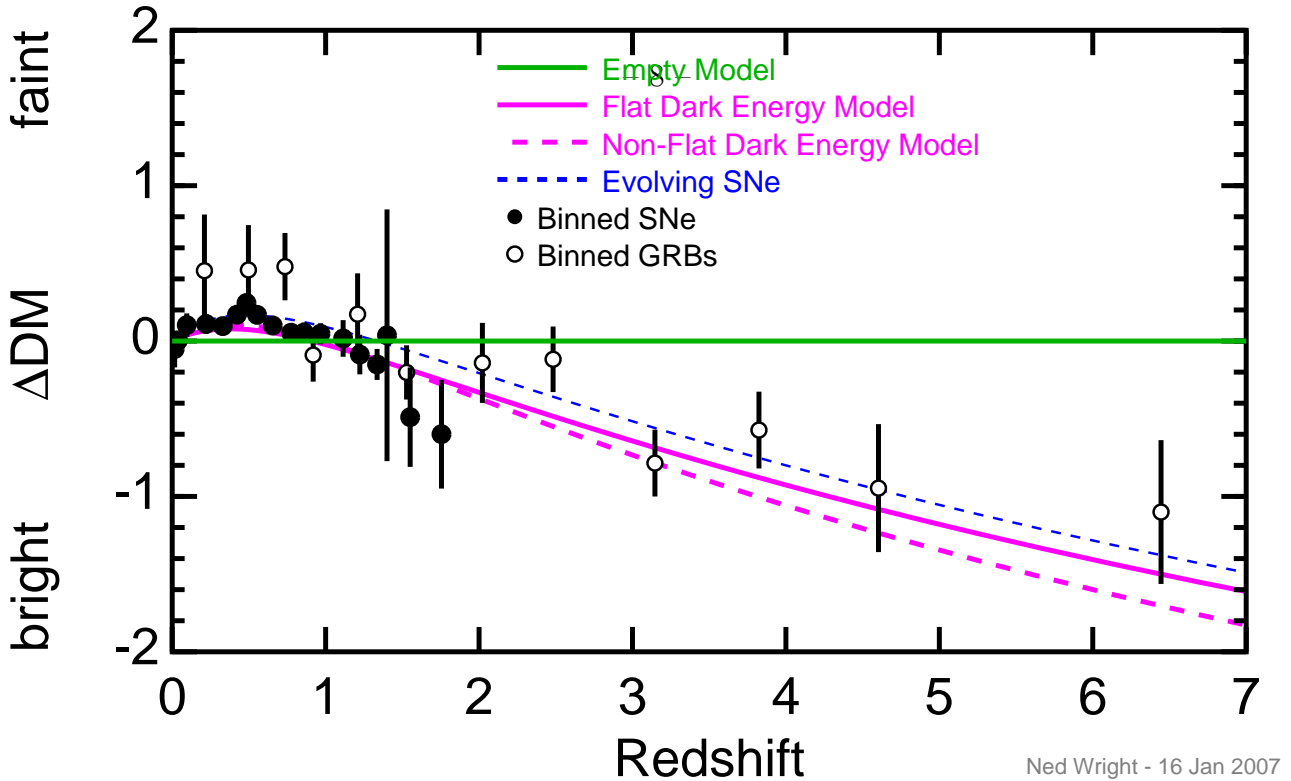
the minimal hierarchical mass pattern gives  $\Omega_\nu/\Omega_M \approx 0.004$  while the WMAP 3 year data give  $n_s = 0.951 \pm 0.017$  (Spergel *et al.* 2006). With these values the corrected weighted mean  $\Gamma$  is  $0.209 \pm 0.014$ .

## 2.6. Acoustic Oscillations

The most important parameter from the CMB data is the acoustic scale. In this paper the stretch parameter  $R$  (Bond, Efstathiou & Tegmark 1997) is not used, but the acoustic scale  $\ell_a$  evaluated at the mean baryon and dark matter densities is used in its place. The acoustic scale is defined as (Page *et al.* 2003)

$$\ell_a = \frac{\pi(1+z_{LS})D_A(z_{LS})}{\int_0^{1/(1+z_{LS})} c_s da/(a\dot{a})} \quad (3)$$

where  $z_{LS}$  is last scattering,  $c_s$  is the sound speed,  $a$  is the scale factor,  $\dot{a}$  is its time derivative, and  $D_A$  is the angular size distance. The stretch parameter  $R$  approximates the denominator



Ned Wright - 16 Jan 2007

Fig. 3.— Binned supernova and GRB data *vs.* redshift compared to a flat  $\Lambda$ CDM model with  $\Omega_M = 0.369$ , and non-flat  $\Lambda$ CDM model with  $\Omega_M = 0.416$  and  $\Omega_{tot} = 1.115$ , and an exponentially evolving model in a  $\Omega_M = 1$  model (Wright 2002).

as  $\propto \Omega_M^{-1/2}$ , which is not a good approximation when the dark energy is significant at  $z_{LS}$ .  $\ell_a$  is very well determined by the CMB data, with  $\ell_a = 303.14 \pm 1.04$  in the non-flat  $\Lambda$ CDM chain. In this paper the full fit to the CMB data is not performed, but the baryon and CDM densities are fixed at their mean values. With this simplification, the determination of the acoustic scale loosens to  $\ell_a = 302.97 \pm 4.14$ . This relative accuracy of  $\ell_a$  with fixed  $\omega_B$  and  $\omega_M$  is the same as the relative accuracy of  $R$ . The main reason to use  $\ell_a$  instead of  $R$  is that it is clear how  $\ell_a$  is modified when the dark energy is important at last scattering.

The second major input involving acoustic oscillations comes from the baryon acoustic oscillations detected by Eisenstein *et al.* (2005). In this paper we use the ratio of the distance  $D_V(0.35)$  at  $z = 0.35$  to the tangential distance at last scattering. This ratio is easily computed even when the dark energy is significant at last scattering. The ratio is also slightly more precise than the  $A$  parameter since the scatter induced by the uncertainty in  $\omega_B$  and  $\omega_M$  cancels out in the ratio. The  $A$  parameter also uses the approximation that the sound travel distance is  $\propto \Omega_M^{-1/2}$  which fails when dark energy dominates early. Finally,  $A/R$  is exactly proportional to  $D_V(0.35)/[(1+z_{LS})D_A(z_{LS})]$ . Using both  $A$  and the distance ratio amounts to double counting the baryon acoustic oscillations.

The redshift of recombination,  $z_{LS}$ , is essentially independent of both the baryon density

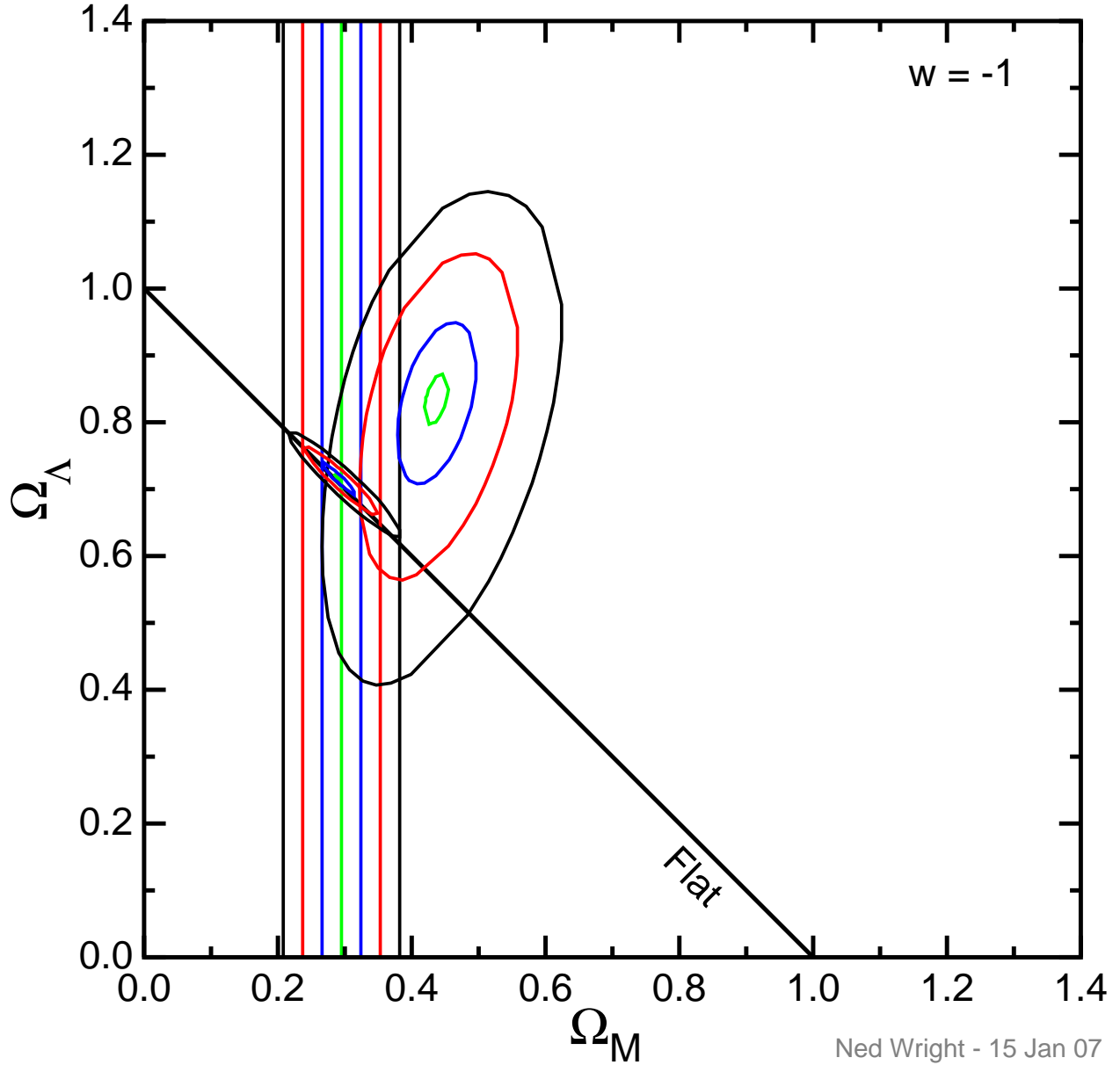
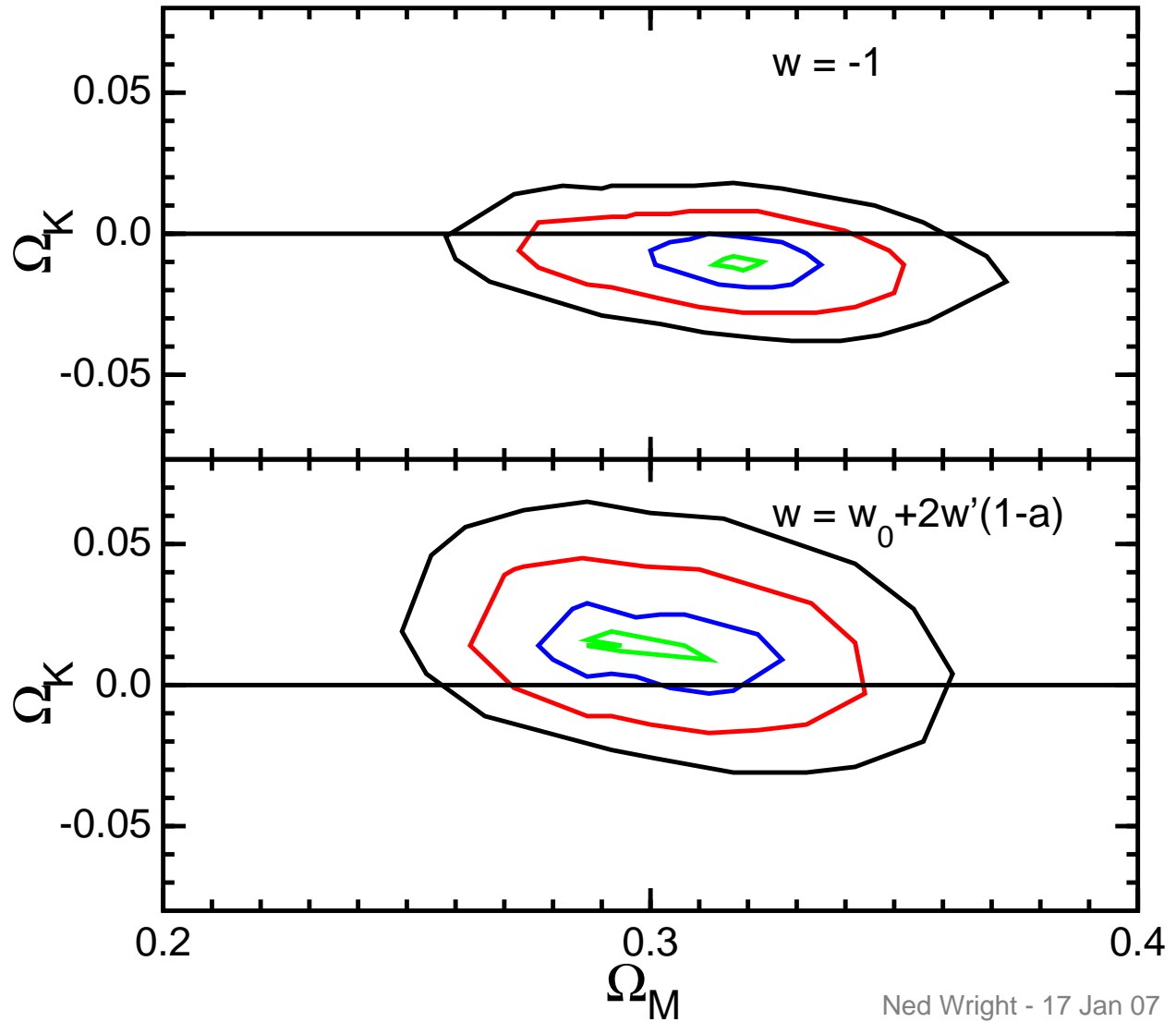
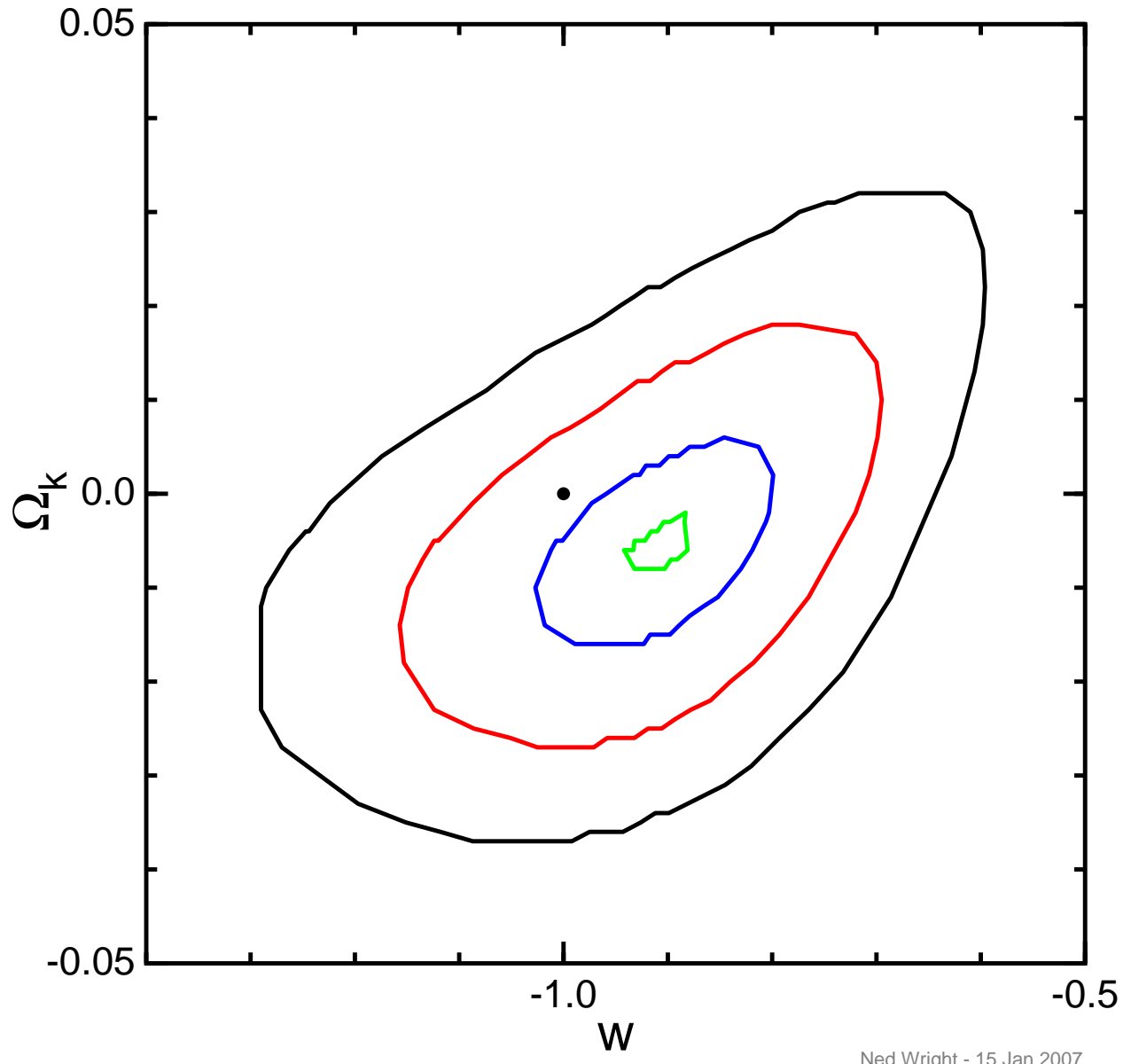


Fig. 4.— Contours of  $\chi^2$  in the  $\Omega_M$ - $\Omega_\Lambda$  plane when the dark energy is assumed to be a cosmological constant with  $w = -1$ . The large ellipses use only the Hubble diagram data from the supernovae and the GRBs. The small ellipses near the “Flat” line use only the CMB acoustic scale and the baryon acoustic distance ratio. Contours are drawn for  $\Delta\chi^2 = 0.1, 1, 4$ , and  $9$ . The vertical lines show  $-3 \dots +3 \sigma$  for the  $\Omega_M$  prior derived from  $\Gamma$ ,  $H_0$  and  $\omega_M$ .



Ned Wright - 17 Jan 07

Fig. 5.— Contours of  $\chi^2$  in the  $\Omega_M$ - $\Omega_K$  plane. In the lower panel the dark energy is allowed to vary as  $w(z) = w_0 + 2w'(1 - a)$ , using all constraints and datasets. A flat model is consistent with the data, and the best fit is very slight open. In the upper panel  $w = -1$ , and a flat model is again consistent but the best fit is slightly closed.



Ned Wright - 15 Jan 2007

Fig. 6.— Contours of  $\Delta\chi^2$  in the  $w$ ,  $\Omega_K$  plane, with  $w'$  fixed at zero and  $\Omega_M$  adjusted to minimize  $\chi^2$  at each point. The black dot shows the flat  $\Lambda$ CDM model, which has 2 fewer free parameters and less than two units of  $\Delta\chi^2$ .

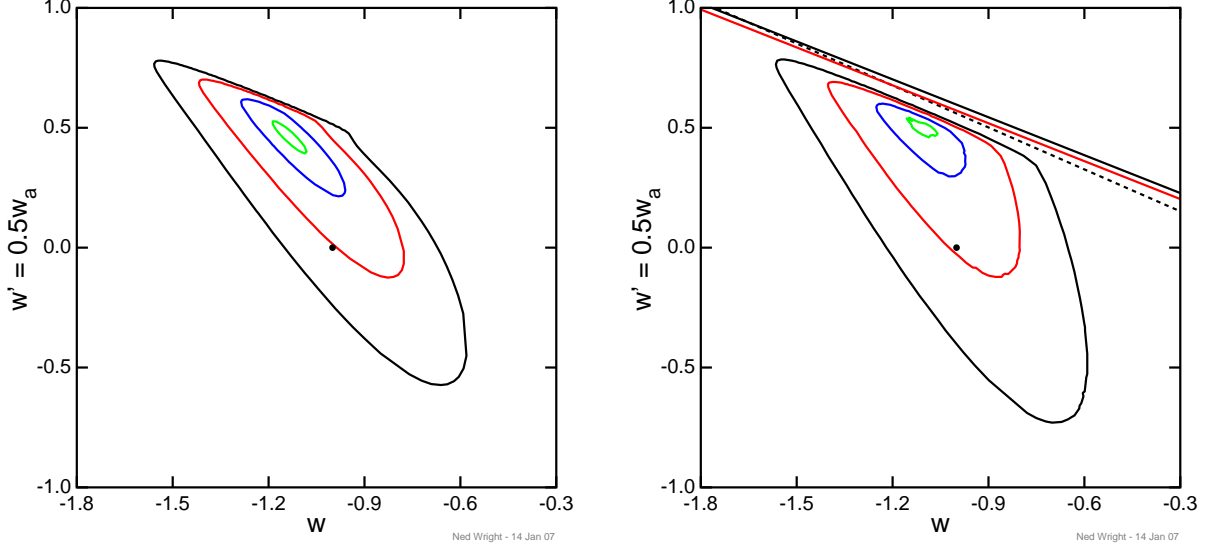


Fig. 7.— Contours of  $\Delta\chi^2$  in the  $w, w'$  plane, using all constraints and datasets. On the left the curvature  $\Omega_K$  is fixed at zero and  $\Omega_M$  is adjusted to minimize  $\chi^2$  at each point. On the right both  $\Omega_M$  and  $\Omega_K$  are adjusted to minimize  $\chi^2$  at each point. The black dot shows the cosmological constant  $w = -1$ . The dashed diagonal line shows where the dark energy is equal to the matter plus radiation density at last scattering. The solid diagonal lines show the 2 and 3  $\sigma$  limits on the Big Bang Nucleosynthesis stretch parameter  $S$ .

and the expansion rate because the electron density is  $n_e \propto H(z)/\alpha(T)$  while the optical depth is  $\tau \propto \sigma_T n_e c/H(z) \propto \sigma_T/\alpha(T)$  where  $\sigma_T$  is the scattering cross-section and  $\alpha$  is the recombination coefficient. Hence  $z_{LS} = 1089$  is used for all calculations in this paper.

## 2.7. Big Bang Nucleosynthesis

Steigman (2006) has analyzed the light element abundances and obtained limits on a stretch factor  $S = (1 + \rho_{DE}/\rho_{\gamma+m+k})^{1/2}$ . The limits are  $S = 0.942 \pm 0.030$ . This means that at 3  $\sigma$  the dark energy density must be less than 6.4% of the radiation density at the redshift of nucleosynthesis,  $z \approx 10^9$ .

### 3. ANALYSIS

All of the analyses in this paper depend on the expansion history and geometry of the Universe. The expansion history can be calculated using

$$\dot{a} = H_0 \sqrt{\Omega_M/a + \Omega_R/a^2 + \Omega_K + \Omega_{DE}[\rho_{DE}(z)/\rho_{DE}(0)]a^2} \quad (4)$$

The dark energy density as a function of redshift is computed using the  $w = w_0 + w_a(1 - a)$  formula (Chevallier & Polarski, 2001). Following Linder (2003) I set  $w' = w_a/2$ . This then gives

$$\frac{\rho_{DE}(z)}{\rho_{DE}(0)} = (1 + z)^{3+3w_0+6w'} \exp\left(\frac{-6w'z}{1 + z}\right) \quad (5)$$

The calculation of angular size and luminosity distances then follows Wright (2006).

Note that the binned distance moduli were not used for the analysis. Thus the Hubble constants used when producing the binned data tables are irrelevant in the analysis. But both the supernovae and the GRBs have an associated “nuisance” parameter,  $\mathcal{M}_{SN}$  and  $\mathcal{M}_{GRB}$ , which are adjusted to give the best modified  $\chi^2$  at every position in the  $\{\Omega_M, \Omega_k, w, w'\}$  parameter space. Thus

$$\begin{aligned} \chi^2 &= \sum_i f((\mu_i - \mu_c(z_i))/\sigma_i) \\ \text{with} \\ \mu_c(z) &= \Delta\mathcal{M} + 5 \log(D_L(z; \Omega_M, \Omega_k, w, w')) \end{aligned} \quad (6)$$

Normally the data on  $\Gamma = \Omega_M h$ ,  $H_0$  and  $\Omega_M h^2$  can be combined to give a prior on  $\Omega_M$ . There is an overdetermined set of equations with variables  $\Omega_M$  and  $h$ :

$$\begin{pmatrix} 1 & 1 \\ 1 & 2 \\ 0 & 1 \end{pmatrix} \begin{pmatrix} \ln(\Omega_M) \\ \ln(h) \end{pmatrix} = \begin{pmatrix} \ln(0.209) \pm (0.014/0.209) \\ \ln(0.1289) \pm (0.0079/0.1289) \\ \ln(0.71) \pm (0.05/0.71) \end{pmatrix} \quad (7)$$

The least squares solution of these equations gives  $H_0 = 67.3 \pm 3.7$  km/sec/Mpc and  $\Omega_M = 0.295 \pm 0.029$ .

But the relationship between  $\Gamma = \Omega_M h$  and the big bend in  $P(k)$  is derived assuming that matter and radiation are the only significant contributors to the density at  $z_{eq}$ , the redshift of matter-radiation equality. Prior to  $z_{eq}$ , the Universe is expanding faster than the free-fall time for matter perturbations, so growth is suppressed for fluctuations that are inside the horizon earlier than  $z_{eq}$ . To allow for the possibility that dark energy contributes,  $z_{eq}$  is found using

$$\Omega_M(1 + z_{eq})^3 = \Omega_R(1 + z_{eq})^4 + \Omega_K(1 + z_{eq})^2 + \Omega_{DE}(1 + z_{eq})^{3+3w_0+6w'} \exp\left(\frac{-6w'z_{eq}}{1 + z_{eq}}\right) \quad (8)$$

The horizon at  $z_{eq}$  is found using

$$D_{eq} = \int_0^{1/(1+z_{eq})} \frac{cda}{a\dot{a}} \quad (9)$$

Then the effective value of  $\Gamma$  is  $(1602 \text{ km/sec})/(H_0 D_{eq})$ . By finding the effective  $\Gamma$  at two different values for  $H_0$ , which leads to two different values for  $\Omega_R$  since  $\Omega_R h^2$  is fixed by the measurement of  $T_0$ , the standard  $\Gamma = \Omega_M h$  can be replaced by a modified power law function of  $h$  which reduces to the standard form except when the dark energy is significant near  $z_{eq}$ . When finding  $\chi^2$ , a weighted mean estimate for  $h$  is found using the  $\Gamma$ ,  $H_0$  and  $\omega_m$  priors. This weighted mean minimizes the  $\chi^2$  contribution from these three priors, and this minimum is added to the  $\chi^2$  from the Hubble diagram, CMB, and the BAO. Therefore  $h$  becomes a third nuisance parameter.

It is simple to find the BBNS  $S$  parameter for any point in the  $\{\Omega_M, \Omega_k, w, w'\}$  parameter space, and add an appropriate term to  $\chi^2$ . Since the desired value for  $S$  is slightly less than one, while dark energy can only increase  $S$ , the BBNS data acts only as an upper limit on  $w'$ , as shown in Figure 7.

#### 4. DISCUSSION

There are a large number of different cuts through the 4 dimensional parameter space that can be plotted, and when different subsets of the data are considered the number of plots multiplies rapidly. Figure 4 shows the  $\Omega_M$  vs.  $\Omega_\Lambda$  plane when the dark energy is constrained to be a cosmological constant with  $w = -1$ . Three data subsets are shown: the supernova and GRB Hubble diagrams, the CMB plus BAO acoustic scale data, and the  $\Gamma$ ,  $H_0$  and  $\omega_M$  data. Clearly the acoustic scale data give a strong confirmation of the need for dark energy, and a much better constraint on the curvature of the Universe. Using all the data together gives the plot shown in Figure 5. The best fit model is slightly closed with  $\Omega_{tot} = 1.011$  and  $\Omega_M = 0.315$ . The best fit flat  $\Lambda$ CDM model has less than one more unit of  $\chi^2$  than the best fit non-flat  $\Lambda$ CDM model so there is no evidence for spatial curvature from these fits. Figure 5 also shows the effect of allowing  $w(z)$  to vary.

Another way to see this is to plot  $\chi^2$  vs.  $w$  and  $\Omega_K$ , as seen in Figure 6. In this plot  $w'$  is forced to zero, and  $\Omega_M$  is adjusted to minimize  $\chi^2$  at each point. This plot is very similar to a comparable plot in Spergel *et al.* (2006).

The flat  $\Lambda$ CDM model has only 5 more units of  $\chi^2$  than a non-flat variable  $w$  model with 3 more free parameters. The probability of this occurring by chance alone is over 16%, so this improvement is not significant.

Plots of the  $w$  vs.  $w'$  plane are shown in Figure 7, with and without the assumption of a flat Universe. The tilted ellipses indicate that the pivot redshifts for these assumptions and the current datasets are  $z = 0.4$  and  $z = 0.22$ . Values of  $w$  at the pivot redshift are close to 0.9 which is the best fit when  $w'$  is forced to zero, as shown in Figure 6.

## 5. CONCLUSION

The current data, even with well over 300 supernovae, is not adequate for measuring a time variable equation of state with reasonable precision. Serra, Heavens & Melchiorri (2007) and Davis *et al.* (2007) agree with this conclusion. The current acoustic scale data, seen in the CMB and the baryon oscillations, is giving more precise information about the expansion history of the Universe, but without the dense redshift coverage provided by the supernovae. There appears to be a systematic deviation of the supernovae data from the models around redshifts near 0.5, whose origin is unknown. Since the choice of data subsets affects the size of this deviation it is probably an artifact. Furthermore the scatter between the distance determinations of identical supernovae by different groups is unexpectedly large. The GRB Hubble diagram is not very precise but it does help break the degeneracy between  $w \neq -1$  and  $\Omega_K \neq 0$ . The 2dF and SDSS values for  $\Gamma$  differ by a slightly disturbing amount. The Hubble constant appears to be well-determined but independent new data would be quite valuable in pinning down  $\Omega_M$  in combination with  $\Gamma$ . Better CMB data from Planck should reduce the uncertainty in  $\omega_B$  and  $\omega_M$ , which will reduce the uncertainty in  $R$  or  $\ell_a$ . It is clear that better data of many types will be needed to pin down  $w(z)$ .

We acknowledge the use of the Legacy Archive for Microwave Background Data Analysis (LAMBDA). Support for LAMBDA is provided by the NASA Office of Space Science.

## REFERENCES

Astier, P., et al. 2006, A&A, 447, 31

Barger, V., Gao, Y., & Marfatia, D. 2006, ArXiv Astrophysics e-prints, arXiv:astro-ph/0611775

Bonamente, M., Joy, M. K., LaRoque, S. J., Carlstrom, J. E., Reese, E. D., & Dawson, K. S. 2006, ApJ, 647, 25

Bonanos, A. Z., et al. 2006, ApJ, 652, 313

Bond, J. R., Efstathiou, G., & Tegmark, M. 1997, MNRAS, 291, L33

Chevallier, M. & Polarski, D. 2001, Int. J. Mod. Phys., D10, 213.

Cole, S., *et al.* 2005, MNRAS, 362, 505

Davis, T. *et al.* 2007, ArXiv Astrophysics e-prints, arXiv:astro-ph/0701510

Eisenstein, D. J., *et al.* 2005, ApJ, 633, 560

Freedman, W. L., *et al.* 2001, ApJ, 553, 47

Linder, E. V. 2003, Physical Review Letters, 90, 091301

Macri, L. M., Stanek, K. Z., Bersier, D., Greenhill, L. J., & Reid, M. J. 2006, ApJ, 652, 1133

Page, L., *et al.* 2003, ApJS, 148, 233

Riess, A. G., *et al.* 2006, ArXiv Astrophysics e-prints, arXiv:astro-ph/0611572

Schaefer, B. E. 2006, ArXiv Astrophysics e-prints, arXiv:astro-ph/0612285

Serra, P., Heavens, A. & Melchiorri, A. 2007, ArXiv Astrophysics e-prints, arXiv:astro-ph/0701338

Spergel, D. N., *et al.* 2006, ArXiv Astrophysics e-prints, arXiv:astro-ph/0603449

Steigman, G. 2006, ArXiv High Energy Physics - Phenomenology e-prints, arXiv:hep-ph/0611209

Tegmark, M., *et al.* 2004, ApJ, 606, 702

Wang, Y., & Mukherjee, P. 2006, ApJ, 650, 1

Wood-Vasey, M. *et al.* 2007, ArXiv Astrophysics e-prints, arXiv:astro-ph/0701041

Wright, E. L. 2002, ArXiv Astrophysics e-prints, arXiv:astro-ph/0201196

Wright, E. L. 2006, ArXiv Astrophysics e-prints, arXiv:astro-ph/0609593